IX CONGRESSO BRASILEIRO DE
ENGENHARIA E CIÊNCIAS TÉRMICAS

9th BRAZILIAN CONGRESS OF THERMAL
ENGINEERING AND SCIENCES

Paper CIT02-0636

WAX BLOCKAGE REMOVAL BY INDUCTIVE HEATING OF SUBSEA PIPELINES

R. Sarmento
Departamento de Engenharia Mecânica, PUC-RIO, 22453-900, Rio de Janeiro RJ
e-mail, rcs@mec.puc-rio.br

G.A.S. Ribbe
Departamento de Engenharia Mecânica, PUC-RIO, 22453-900, Rio de Janeiro RJ
e-mail, gribbe@chromax.com.br

L.F.A. Azevedo
Departamento de Engenharia Mecânica, PUC-RIO, 22453-900, Rio de Janeiro RJ
e-mail, lfaa@mec.puc-rio.br

Abstract. *Total blockage of subsea petroleum production lines due to wax deposition is a relevant problem for the industry. This problem has led to significant capital losses associated with the loss of production and the substitution of plugged lines. The present paper is a study of the feasibility of a remediation procedure aimed at helping the removal of wax plugs. In this procedure, the section of the oil line plugged with wax is inductively heated by means of an external coil positioned over the line at sea bed. The objective of the work is to estimate the level of electrical power required to soften the wax plug inside the line. To this end, a transient heat conduction model was employed to predict the temperature distribution in the line wall and solid wax. This information was employed to estimate the basic dimensions of the heating coil section and thermal insulation employed to minimize the heating losses to the cold sea water environment. A laboratory experimental study with a subsea pipeline section plugged with wax was conducted to verify the numerical model predictions and to test the performance of the inductive heating coil.*

Key-words: *wax removal, subsea pipelines, inductive heating*

1. Introduction

The world economy still depends heavily on petroleum production. Nearly half of the sedimentary basins that offer good prospects of finding petroleum are located offshore, at long distances from the coasts. Today, the most active offshore production areas are the Gulf of Mexico, the North Sea, China Sea, West Africa and the coast of Brazil. The drive toward production at deep waters in these areas is evidenced by the data available on the water depth records established in subsea petroleum production wells. In 1983 the record was 208m, while in 2000 production at a water depth of 1853 m was achieved (Machado, 1999). The production at elevated water depths, such as those just mentioned, involves specially designed equipment and costly, complex operations. Even so, due to the steady investment in technology, the cost of production of the petroleum barrel has dropped steadily. For instance, in the Campos Basin in Brazil the price of the oil barrel produced has decreased from US$ 16.74 in 1989 to US$ 5.92 in 1997 (Machado, 1999).

Among the several challenges in deep water petroleum production, the deposition of wax in the interior of production and transportation pipelines is one of the most critical operational problems faced by the industry. The crude oil flows out of the reservoir at, typically, 60 ^{0}C into the production pipelines. These lines carry the oil to the platforms and from the platforms to shore. At elevated water depths, the ocean temperature is of the order of 5 ^{0}C. The solubility of wax in the oil is a decreasing function of temperature. As the oil flows, it loses heat to the surrounding water. If a certain critical temperature level is reached, the wax may precipitate off solution and deposit along the inner walls of the pipeline. The accumulation of the deposited material may lead to increased pumping power, decreased flow rate or even to the total blockage of the line with loss of production and capital investment.

There are traditional methods of prevention of wax deposits employed by the industry. These methods include, among others, the use chemical inhibitors, thermal insulation and heating of the lines by electrical or chemical means. The cost of utilization of these methods, however, increases steeply with water depth, being crucial to the economical viability of offshore petroleum production.

Once wax deposition has occurred, a common strategy is to employ pigs to mechanically remove the wax layer. Pigs are devices that are introduced into the pipeline with a tight fit, being driven by the flowing fluid. The mechanical stresses developed between the pig and the pipe wall should be sufficient to remove the deposited wax.

The passage of a pig is a critical and risky operation. Normally the operators tend to perform a wax removal operation using a series of pigs with increasing hardness or oversize. The objective of this strategy is guarantee that small amounts of wax are removed at each passage of the pig. If a pig removes a large amount of wax at once, there is a

large risk that the removed wax will agglomerate downstream of the pig, forming a plug of elevated mechanical strength. In this case, the pig gets stuck and the line plugged. A common strategy employed to try to unplug the line is to increase the pressure upstream of the pig to values close to the maximum value allowed for the line. When this pressure increase operation fails to loosen the pig, the result is that the removed wax is compacted, forming a nearly solid plug of several meters in length and of high mechanical strength that totally blocks the line. When this critical situation is attained, there is a small chance of recovering the line, and the line is normally abandoned. When the line is completely blocked, it is not possible to flow chemicals to the blockage location to try dissolving it. In case the blockage is located in a vertical section of the line, it is possible to use dense solutions that would reach the blockage location by gravity settling. This technique has been employed with success utilizing chemicals that react exothermically at the wax blockage location, melting it (Khalil et al., 1994).

The cost of a subsea production line is elevated, and justifies a continued research effort directed to the development of techniques for restoring the flowing conditions of a blocked line. A first and critical step that needs to be addressed prior to any attempt of unplugging the line, is to locate the blocked region. Subsea production lines are normally long, typically in the range of 1 to 10 km, and locating a wax plug of a few meters in length is a complex task. Pressure-echo techniques have been developed and employed successfully in recent years (Kuchpil, 2001). In this technique, the plugged line is connected to a pressure vessel containing pressurized fluid. A valve connecting the vessel to the line is activated rapidly, in order to produce a pressure wave that travels along the line. The pressure wave reflects at the blockage region and travels upstream along the line. A pressure transducer installed in the line monitors the time between the passage of the original pressure wave and the reflected wave. The knowledge of the time of transit of the pressure wave and the velocity of propagation of the sound in the fluid allows the calculation of a good estimate of the location of the blocked region. The uncertainty of this technique is limited by the knowledge of the sound speed. It is not uncommon that a mixture of liquids and gases be present in the line increasing the uncertainty in the estimate of the sound speed.

Other technique for locating the blocked region relies on the measurement of the change in external diameter of the line when submitted to elevated internal pressure (Kuchpil, 2001). A special tool equipped with a caliper and a video camera is used by a remotely operated subsea vehicle to measure the external diameter of the line. Upstream of the blocked region a variation of diameter is felt when the line is pressurized. Downstream of the blockage no appreciable variation of diameter is sensed when the line is pressurized. By changing the position of the caliper tool it is possible to locate the blockage with good accuracy.

Once the blockage is located, the line can be suspended and repaired by special boats in a normally costly operation. An alternative is to try to melt the wax plug with the line at sea bed. The present paper is a study of the technical viability of using inductive heating to melt the wax plug of a subsea line.

2. The inductive heating configuration

Subsea production lines can be rigid or flexible. Rigid lines are made of series of welded steel pipes. Flexible lines are made of several layers of different materials, each having a specific function. Flexible lines are widely used in the subsea arrangements employed in the Campus Basin in Brazil. Figure 1 presents a photograph of a typical flexible line. Seven layers can be seen in the figure. The inner most layer is a stainless steel spiral that contacts the flowing oil. A polymeric material constitutes the second layer providing sealing for the stainless steel spiral. The third layer is a carbon steel spiral layer designed to provide mechanical strength to the line. A tape layer is used to decrease friction between the third and fifth steel layers. The fifth and sixth layers are counter-wound, carbon steel spirals that provide mechanical resistance against longitudinal loads. The outermost layer is made of polymeric material and provides sealing against the sea water.

In the configuration proposed, a coil is placed on the external part of the line, over the plugged region, and fed by an alternate current. It is expected that the current induced in the metallic layers of the line will produce sufficient energy to heat the solid paraffin in the interior of the line to a temperature close to its melting point. A pressure difference applied across the wax plug would, then, be able to move the plug, restoring the line to operation.

Figure 1 – Typical structure of a subsea flexible line.

Inductive heating of metallic parts is widely used for metal processing in applications such as melting, heat treating, welding and pre-heating for metal forming (Zinn and Semiatin, 1988). In the specific case of heating of flexible lines, there are challenges to be addressed. Firstly, the spiral structure of the metallic layers that compose the flexible line is not ideally suited for conducting the induced currents. Secondly, the presence of layers of polymeric materials in the structure of the line imposes relatively low limits to the maximum temperature attained by these layers. On the other hand, inductive heating should be sufficient to heat the solid wax plug to temperatures close to the wax melting temperature. For instance, a temperature level of around 60°C is necessary to soften the wax plug, while a maximum temperature of 90°C should not be exceeded in order not to allow melting or deformation of the polymeric layers. As can be seen, there is a narrow temperature window to successfully apply the inductive heating method analyzed in the present paper. This narrow operating range requires a careful study of the heat transfer characteristics of the heated line in a cold subsea environment. The only work found in the literature related to the use of induction for heating installed flexible subsea pipelines is focused on the electromagnetic aspects of the problem and does not address the thermal behavior of the heated line (Dittz, 2001).

The research program reported in the present paper has two major objectives. The first objective is to prove that wax in the interior of flexible lines can be heated by induced currents in the metallic layers. The second objective is to verify what is the necessary level of thermal energy that needs to be transferred to the wax plug in order to bring its temperature close to its melting point. An experimental and numerical program was developed to attain these objective, as will be described next.

3. The test section

An experimental test section was constructed with the objective of verifying the technical feasibility of inductively heating a solid wax deposit contained in a commercial subsea flexible line. Figure 2 is a schematic view of the test section constructed.

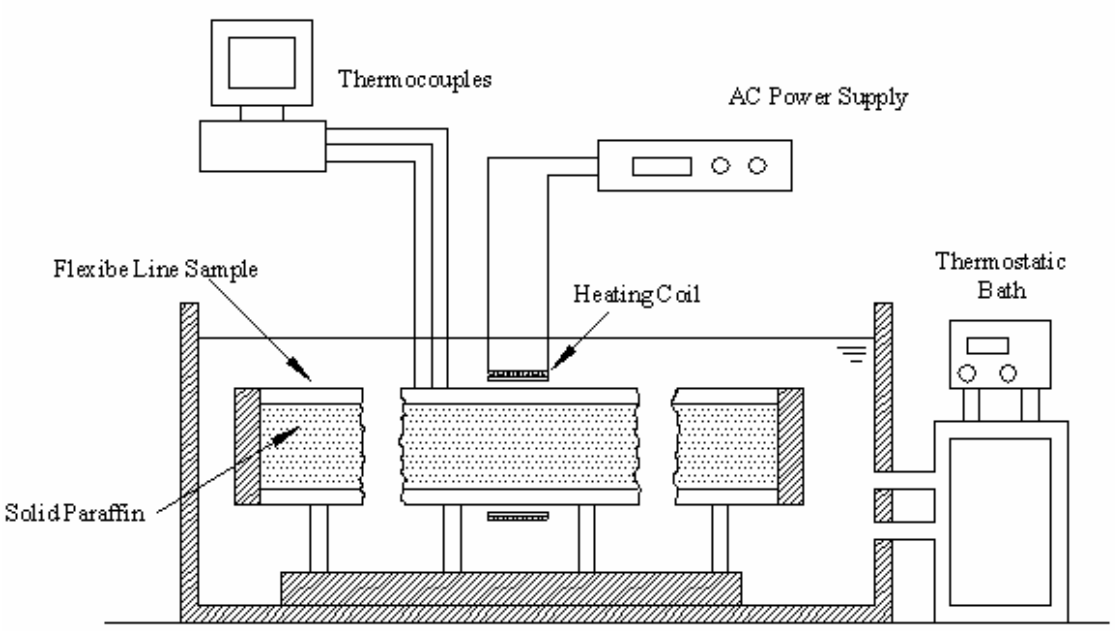

Figure 2 – Schematic view of the experimental test section.

A 800-mm-long piece of a 100-mm internal diameter flexible line was used in the laboratory tests. The particular line used in the tests was formed by an inner stainless steel spiral layer covered with a polymeric layer, two counter-wound, spiral carbon steel layers, a plastic tape and an outer polymeric layer. In some experiments, a rubber external insulation layer was added. The dimensions and thermophysical properties of each layer are presented in Table 1. Reference should be made to Fig. 3 for the nomenclature of the radial positions of the layers.

Two Polypropylene caps where specially machined to serve as plugs for the two ends of the flexible line sample. These plugs provided water seal that kept the outside cooling water from penetrating the interior of the line. The Polypropylene caps had also the function of holding a 6-mm diameter Celeron rod that was positioned at the centerline of the flexible line (not shown in the figure). This rod was used to support several thermocouples used to sense the paraffin temperature history. The thermocouples were installed in small holes drilled in radial Celeron rods (3-mm diameter) that were fixed in holes drilled on the central rod. This arrangement allowed the accurate positioning of the thermocouples in the interior of the line. Ninety, pre-calibrated, 0.125-mm-diameter, Crommel-Constantan thermocouples were installed in the Celeron rods.

Table 1 – Geometric and Thermophysical Properties of the Plugged Line

Material	Radial Position (mm)	Thermal Cond. k [W/m.K]	Density r [kg/m^3]	Specific Heat c_P [J/kg.K]
Paraffin	R =50.8	0.24	900	2900
Stainless Steel	r_2= 53.5	13	8240	468
Internal Polymeric layer	r_3 = 58.5	0.16	1190	2000
Carbon Steel	r_4 = 64.5	60	7850	440
External polymeric layer	r_6 = 70.0	0.23	1140	1700
Rubber Insulation	r_7 = 120.0	0.1	1100	2000

Commercial grade paraffin was used in the tests. The paraffin had a melting point in the 53-56^{o}C range. The flexible line with the thermocouple assembly mounted was positioned vertically for the introduction of the paraffin. The lower end was closed with the Polypropylene cap, while the other end was kept open. A rod-type electrical heater was introduced in the line. The solid paraffin, previously grinded in small flakes, was introduced in the line over the electrical heater. While the melted paraffin occupied the bottom part of the line the heater was removed and the paraffin allowed to solidify. This operation was repeated several times until the line was completely filled with solid paraffin. This step-by-step filling operation guaranteed that no air pockets were trapped in the paraffin during solidification. The top end of the line then was closed with the Polypropylene cap.

The line section containing the solid paraffin was placed horizontally on supports in a Plexiglass tank with dimensions of 1000 x 400 x 500 mm (length x width x height). The tank was filled with water and connected to a thermostatic bath and water-circulating unit. The temperature of the water was maintained at 5^{o}C during all the tests, a temperature similar to that encountered in deep water operations. The tank was thermally isolated with 25-mm-thick Styrene plates. The thermocouples were connected to a Agilent model 34970A data acquisition unit.

The heating coil was formed by 147 loops wound around a 150-mm diameter, 150-mm long PVC pipe. The coil was fabricated with enamel-coated, 1-mm diameter copper wire. The coil was positioned at the center of the flexible line, supported by small Styrene spacers. The level of the water in the tank was such that covered both, the flexible line and the heating coil.

3.1. The test procedure

An autotransformer was used to supply alternate current to the coil. The power supplied by the coil to the flexible line was calculated by subtracting the power supplied to the coil without the flexible line installed from the power measured with the line installed, maintained the same current. The difference in power was the power absorbed by the line.

The experimental test procedure was initiated by letting the flexible line filled with solid paraffin attain thermal equilibrium with the water circulating in the tank. After that period, a particular power level was adjusted in the autotransformer. The temperature of the paraffin was monitored by the readings of the data acquisition unit, so that the melting temperature of the paraffin was never reached. If the rise of the temperature sensed by the thermocouples indicated a possibility of attaining the paraffin melting temperature, the power to the coil was switched off and the data run aborted. The paraffin was allowed to attain thermal equilibrium with the water, and a new lower value of the power was set at the autotransformer.

4. Numerical simulations and the validation experiments

The experiments described in the previous section employed samples of flexible lines of short dimensions due to the limitations of the laboratory tests. In order to study the feasibility of the inductive heating technique, it would be necessary to have the capability of studying the thermal behavior of much longer lines. To this end, a transient heat conduction model for the line and the solid paraffin deposit was implemented, as will be described in the present section.

Accurate solutions of transient heat conduction problems are relatively easy to be obtained with current numerical techniques and computer hardware. This would be true for the present problem if it were not for the uncertainty on the knowledge of the thermophysical properties of the materials needed for the calculations. Indeed, the values of the thermal conductivity and heat capacity for the materials that compose the several layers of a commercial flexible line were not available. The construction of the flexible line employs spiral layers of carbon and stainless steel, together with layers of polymeric materials of different types. The contact resistance between these layers is not known and may play a significant role in the overall thermal behavior of the line. Another point of concern is the uncertainty on the thermal properties of the paraffin employed in the tests. Further, the type of thermal contact between the paraffin and the innermost spiral layer of the flexible line obtained with the melting procedure used to fill the line is not known.

In view of these uncertainties, a set of experiments was conducted to validate the numerical solutions. Since the spatial distribution of the power transferred to the steel layer of the flexible line by the induction coil is not known, a resistive heating element was employed to heat the line. This heating element was fabricated by winding a 1-mm-diameter, enamel coated copper wire around the external face of the carbon steel layer of the line. To do that, a portion of the outermost polymeric layer of the line was cut and removed, exposing the steel layer. After the copper wire was

installed, the polymeric layer was fit back into its original position, covering the copper wires. The total length covered by the copper wires was 150 mm. Power to the copper wires was provided by a DC power supply, so that no inductive heating was possible.

Figure 3 presents a schematic view of the flexible line filled with solid paraffin and was prepared to aid in the description of the numerical model developed. The figure is not drawn to scale, and represents a four-layer line filled with paraffin. According to the figure, region 1 represents the solid paraffin, region 2 a stainless steel layer, region 3 an inner polymeric layer, region 4 a carbon steel layer and region 6 an external polymeric layer. Region 5 represents the copper wire winding used as the resistive heater for the validation tests. That is the region to where the volumetric heat generation was assigned. This region is not present in the case of inductive heating simulations. In the case of inductive heating, the volumetric heat generation was assigned to a segment of region 4, the carbon steel layer. Region 7 represents a rubber layer used for providing additional thermal insulation for the line.

The transient, heat conduction equation can be written as,

$$\partial(\rho\, c\, T)/\partial t = \mathbf{div}\left[k\, \mathbf{grad}\, T \right] + q''' \tag{1}$$

In the above equation, T is the temperature and t the time. For each material of the line, ρ is the density, c the specific heat and k the thermal conductivity. The heat generated per unit volume is q'''. A convenient dimensionless form of the equation can obtained with the following dimensionless parameters: $r^* = r/R$, $x^* = x/R$, $\rho^* = \rho/\rho_{ref}$, $c^* = c/c_{ref}$, $k^* = k/k_{ref}$, $\alpha_{ref} = k_{ref}/\rho_{ref}\, c_{ref}$, $t^* = \alpha_{ref}\, t/R^2$, $\theta = k_{ref}\,(T-T_\infty) / q_o''' R^2$. In the definition of the dimensionless parameters, r and x are the radial and axial coordinates, R is the internal radius of the line, T_∞ is the external water ambient temperature and q_o''' is the heat generated per unit volume at the beginning of the experiment.

For the case depicted in Fig. 3 that represents the insulated line heated resistively, the use of the dimensionless parameters suggested in the heat conduction equation and in the initial and boundary conditions reveals that the problem is governed by 31 dimensionless parameters. These are six dimensionless radius, three dimensionless lengths, three sets of seven dimensionless properties (ρ, c and k) and a Biot number representing the dimensionless convective heat transfer from the line to the water, that is, hR/k_{ref}, where h is the convective heat transfer coefficient. In view of the large number of dimensionless parameters, a complete parametric study of the problem is not feasible. Instead, only some typical configurations and operating conditions will be studied in the present work.

The heat conduction equation together with the appropriate initial and boundary conditions were solved by a finite volume technique (Patankar, 1998). The equation was discretized using implicit time integration and employing a central difference scheme to evaluate the heat fluxes at the control volume faces. The algebraic system was solved by a TDMA line-by-line algorithm. A non-uniform mesh was used to better resolve the expected steeper temperature gradients at the interface of the several materials that compose the line. Typically, a 82 x 82 mesh was employed in the calculations.

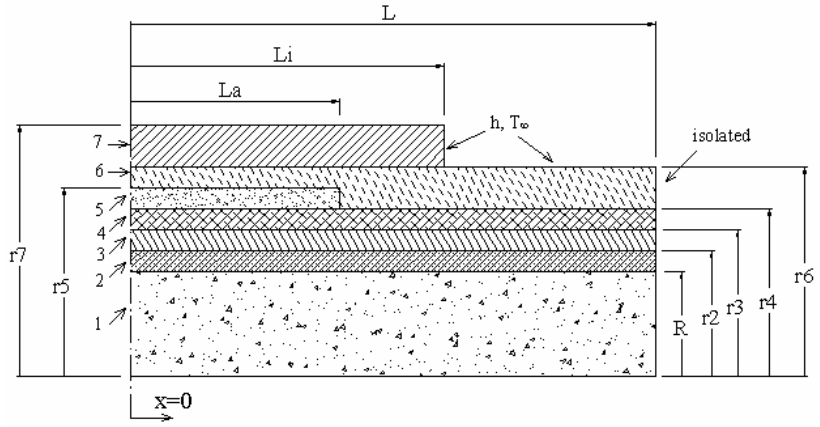

Figure 3 – Cross section view of the flexible layer. Not drawn to scale.

5. Results and discussion

5.1. Validation results

We start the presentation of the results obtained by discussing the experiments conducted with the resistive heating test section prepared to validate the numerical solutions. Figure 4 presents a comparison of experimental and numerical results for a power level of 100 W. Several other power levels ranging from 30 to 150 W were tested during the experiments. Power levels higher than 100 W yielded temperatures at the paraffin-flexible line interface higher than the melting point of the paraffin. As mentioned before, experiments that led to temperatures higher than the paraffin melting point were aborted. Results for power levels other the 100 W are not presented here due to space limitations.

In Fig. 4, the temperature is presented as a function of the dimensionless axial coordinate x/R, for a radial position located at the centerline of the flexible line, where the solid paraffin is present. This position corresponds to a dimensionless radial coordinate r/R = 0. The temperature profiles are presented for six selected times, counted from the beginning of the heating period. The experimental results are represented by the symbols, while the dashed lines represent the predictions of the numerical simulation. The lowermost dashed line corresponds to 1.3h, while the line above that corresponds to 3.3h. The upper most curve represents three coincident solutions for 12.7, 14.7 and 16.7h.

As can be noted in the results presented in the figure, the flexible line and the solid paraffin are initially in thermal equilibrium with the external cooling water maintained at 5^{o}C. After approximately one hour, the temperature distribution exhibits a maximum at the central section of the line (i.e., x/R = 0) of approximately 12 ^{0}C above the initial temperature. A steady state condition is attained after approximately 12 hours. The level of temperature attained at the center of the solid paraffin is of the order of 43^{o}C, sufficient to soften the solid deposit in the case of a field application. The results presented indicate that the axial diffusion of heat through the solid paraffin and through the layers that compose the line is not significant. Indeed, it can be noted that a significant temperature increase is only obtained within a limited region under the heating section. The heating section is located in the region delimited by -1.5<x/R<1.5 (only the positive region is presented in the figure). Out of this region the steady state temperature of the centerline drops sharply due to the loss of heat to the surrounding water. This finding indicates that, in a field application with no use of any additional external insulation, heating of the of the solid paraffin within the line will only attain the desirable temperature levels if the heating section covers most of the solid paraffin region.

An observation of Fig.4 indicates that the numerical solutions for the longer times agree reasonable well with the experiments for the heated region (r/R<1.5). Out of this region the numerical results over predict the temperature distribution. This is probably due to the spiral nature of the metallic layers of the line that are not homogeneous solids, as assumed by the numerical model. The assumption of a homogeneous solid layer overestimates the axial diffusion of heat. For shorter times, the numerical solutions tend to under predict the temperature distribution in the heated section, with the deviations decreasing for longer times. It should be noted that the level of agreement between experiments and computations was obtained by using the thermophysical properties for the paraffin and the materials that compose the flexible line presented in Table 1. These values were obtained from standard textbooks and handbooks (e.g., ASHRAE, 1981 and Incropera and DeWitt, 1990). No attempt was made to adjust the properties of the materials to obtain a better agreement with the experiments. The value of the external convective heat transfer coefficient used as a boundary condition for the external surface of the line in contact with the water was taken as 300 W/m^{2o}C, representing water in natural convection over a cylinder (Incropera and DeWitt, 1990). It is believed that a better level of agreement would be obtained if the thermal properties of the materials were known with higher accuracy.

Figure 5 displays the steady state axial temperature distribution for different radial positions, r/R, within the solid paraffin and within the external and internal polymeric layers of the flexible line. The power level delivered to the resistive wire was again 100 W. The predictions of the numerical solutions are presented in the figure as solid, dashed

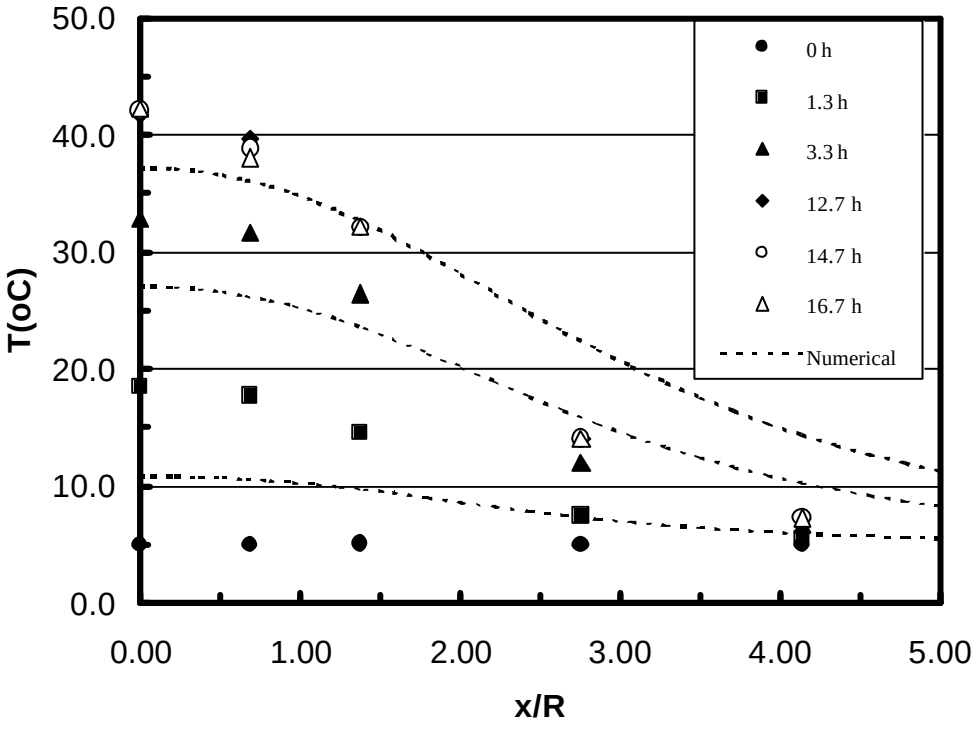

Figure 4 – Transient axial temperature distribution at the flexible line centerline (r/R =0). No insulation. Resistive heating at 100 Watts. Dashed line represents numerical solutions.

and shaded lines. It should be noted that the temperature distributions presented for the radial positions located within the line external and internal polymeric layers were obtained solely by numerical simulations, since no thermocouples were installed within the wall of the line. This was due to technical limitations that did not allow an accurate drilling through the steel layers to install the thermocouples.

The radial variation of the temperature profiles presented in Fig. 5 offers good insight into the temperature levels prevailing in each layer. For instance, the results show that there is little radial variation of the temperature in the paraffin for all axial locations measured. At the paraffin/line wall interface (r/R = 1) the maximum temperature attained is of the order of 46^0 C which, in a field application, would be sufficient to soften the paraffin plug and allow its removal by an applied pressure differential across the plug. However, the sharp drop of the interface temperature outside the heating region is evident, as already seen in Fig.4 for the centerline temperature. This, again, is an indication that the movement of the solid plug would not be possible, and that heating along the whole length of the obstruction would be necessary. Worth noting in Fig. 5, is the nearly perfect axial symmetry of the temperature profiles, indicating that the experimental test section was carefully constructed and operated.

An analysis of the numerically predicted temperature distribution inside the flexible line polymeric layers is important to define the operating power level. As already mentioned, the polymeric layers do not stand temperatures above a certain level without deteriorating. For the case of the line sample employed in the experiments, the maximum temperature allowed for the outer polymeric layer and the interior polymeric layer is of the order of 90^oC. The predictions presented in Fig.5 show that this level of temperature is never achieved in the experiments conducted with the power level of 100 W. The simulations also show that the temperature of the external polymeric layer is higher than the inner polymeric layer, since the external layer is closer to the heating region.

The influence of the presence of a layer of insulating material on the temperature distribution in the flexible line can be assessed with the help of Fig. 6. For the experiments and numerical calculations related to Fig. 6, an additional insulating layer was placed around the external surface of the flexible line. A 50-mm-thick, closed pore, rubber foam was used (thermal conductivity of approximately 0.1 $W/m^2\ ^oC$). The length of the insulating layer was the same as the resistive heating section, that is, 150 mm. The power level employed was 100 W.

In Fig. 6, the experimental and numerically determined axial temperature distributions are presented for five radial positions within the paraffin, including the flexible line centerline (r/R = 0) and the paraffin/wall line interface (r/R = 1). Temperature is also presented for radial positions at the external (r/R = 1.1) and internal polymeric layers (r/R = 1.32). As mentioned before, experimental data are not available for the external layer. For comparison purposes, a curve fit of the experimental results of Fig. 5, corresponding to the paraffin/wall interface temperature distribution for the non-insulated case, is presented as a shaded line.

The results presented in Fig. 6 show that, for steady state conditions, the insulation not only increases the temperature level of the paraffin and the line layers, but also increases the axial heat diffusion. This can be verified by the flatter axial temperature profile under the insulated region ($-1.5<x/R<1.5$), as compared to the non insulated case.

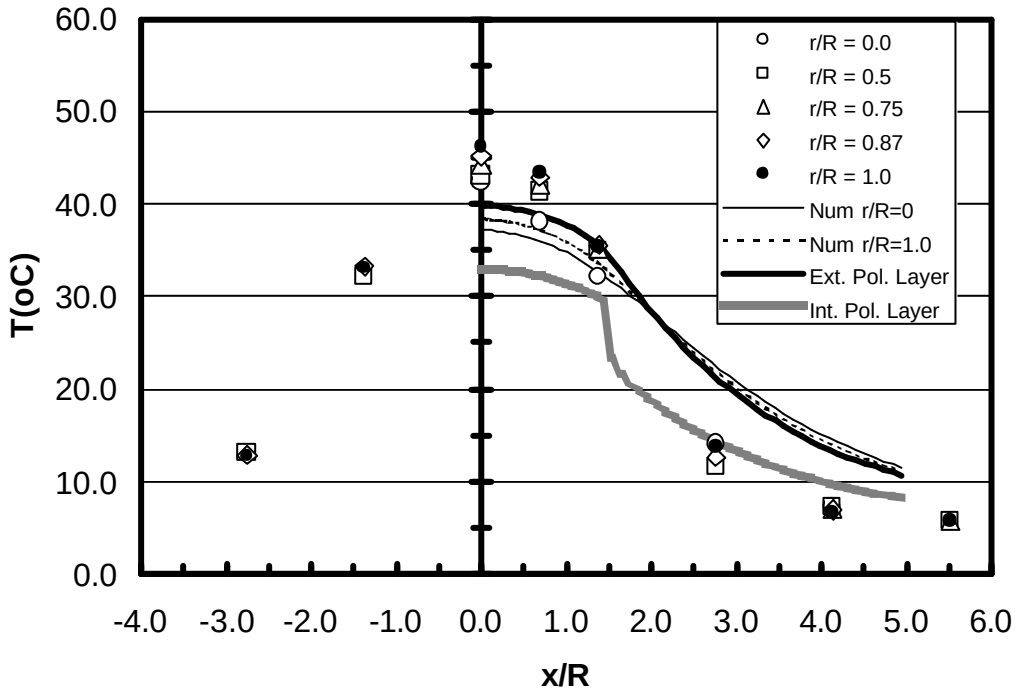

Figure 5 – Steady state axial temperature distribution for different radial positions. No insulation. Resistive heating at 100 Watts. Solid, dashed and shaded lines represent numerical solutions.

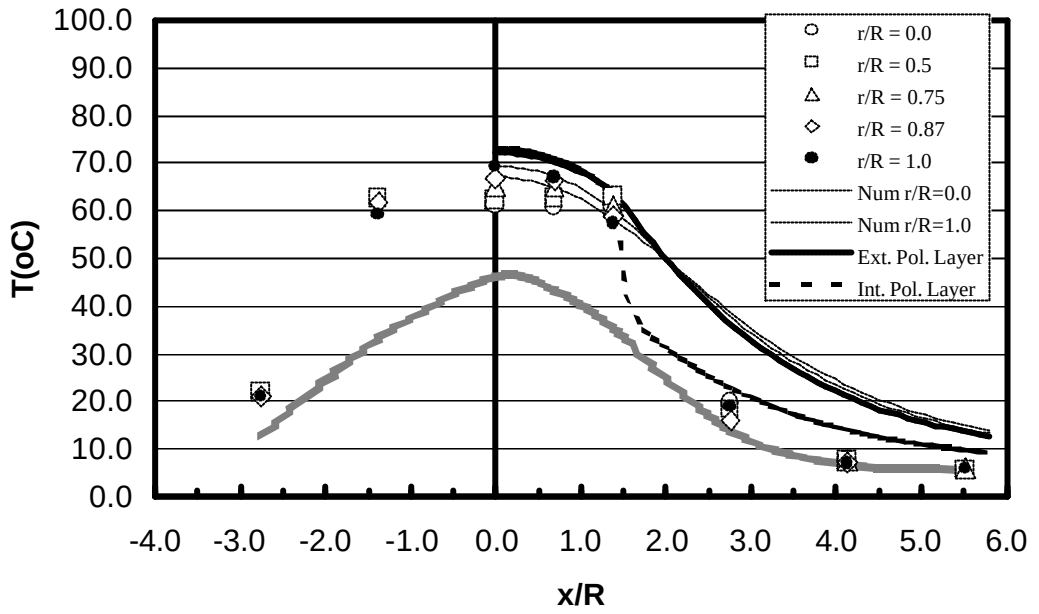

Figure 6 – Steady state axial temperature distribution for different radial positions. With insulation. Resistive heating at 100 Watts. Shaded line represents experiments for r/R=1.0 without insulation.

This is a positive effect for the purpose of removing the paraffin plug, and would be expected since the heat transfer to the surrounding water is decreased by the use of additional insulation. Out of the insulated region, a sharp decrease in temperature is verified, as in the non-insulated case. The results presented indicate that longer lengths of insulation could extend the axial heated length of paraffin. Results for longer insulations are presently being investigated in our laboratory. Numerical studies for longer insulation will be presented shortly in this paper.

The comparison of numerically and experimentally predicted results is very good for the heated region. Indeed, at the heated region for r/R=0 and r/R = 1.0 both results agree remarkably well. Out of the heated region, the numerical results over estimate the temperature distribution, as in the non insulated case. The numerically predicted temperature profiles for the internal and external polymeric layers indicate that under the heated and insulated region both layers display the same temperature. Out of the heated region the temperature of the internal polymeric layer drops sharply.

5.2. Inductive heating results

Figures 7 and 8 were prepared to present the results obtained with the induction heating coil described in the experiments section of this paper. The power level delivered by the AC power supply to the heating coil was equal to 470 W, but only 190 W (approximately 40 %) were effectively dissipated in the steel layer of the flexible line. This value was obtained by subtracting the power delivered without the flexible line installed from the power delivered to the coil with the flexible line installed, for the same current level, as mentioned in the description of the experimental procedure employed in the experiments.

Figure 7 presents the transient response of the axial temperature distribution at the centerline of the flexible line where it can be verified that a steady state condition is attained after, approximately, 10 hours. The main information conveyed by Figs. 7 is the fact that heating the solid paraffin inside a commercial subsea flexible line by means of an inductive coil is, in principle, a viable technique. Indeed, the level of steady state temperature attained at the center of the paraffin is within the range of that expected to soften the paraffin and allow its removal. Other power levels were tested as part of the experimental program but are not presented here due to space limitations. It should be mentioned that in some cases of higher power settings, levels of temperature above the melting point of the paraffin were obtained and, because of that, the experiments were aborted. While heating of the paraffin was obtained, it is evident from the figure that the levels of temperature attained by means of inductive heating with the power level of 190 W are lower than those obtained with the resistive heating experiments at 100W. This fact can attributed to the distinct spatial distributions of the power delivered in the two heating modes. In the case of the resistive heater, the total power delivered is distributed over the well defined volume formed by the copper heater wires. For the inductive heater, the volume where the induced currents are acting is not precisely known. It is certain, however, that the currents are induced in the carbon steel layers of the flexible line, which have larger volumes than that of the copper wires of the resistive heater. As a consequence, the power dissipated per unit volume, q''', is lower for the inductive heating case, implying in lower temperature levels in the line. The widening of the heated region can be observed by the smother temperature gradients verified at the edge of the inductive coil (x/R > 1.5), as compared to the resistive heated case of

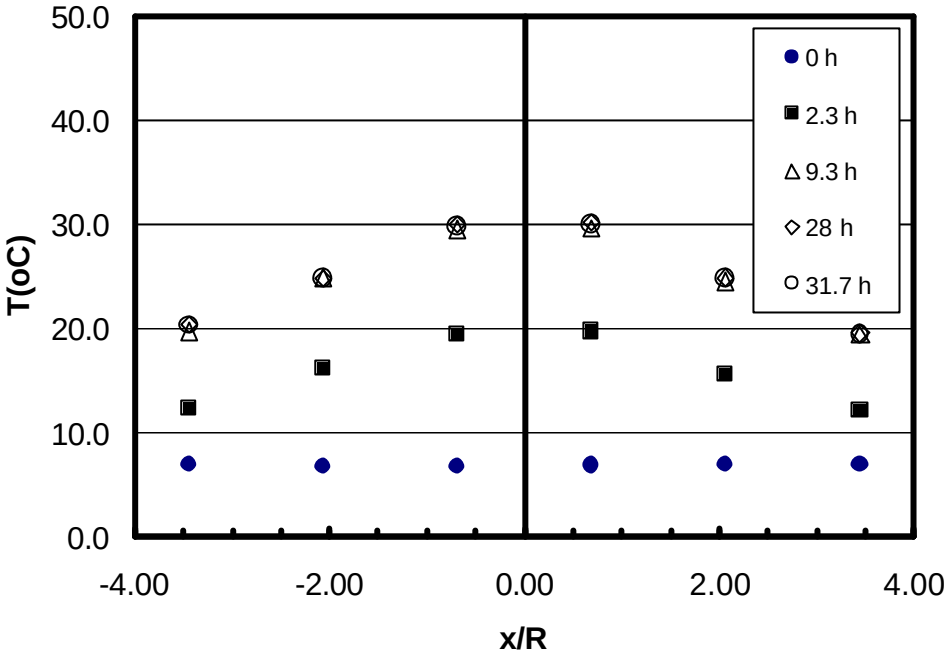

Figure 7 – Transient axial temperature distribution at the flexible line centerline (r/R =0). No insulation. Inductive heating at 190 Watts.

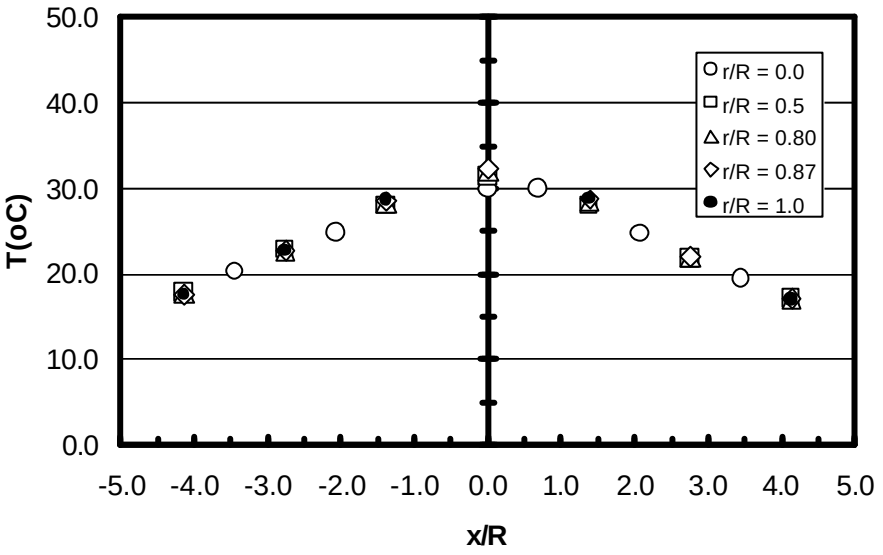

Figure 8– Steady state axial temperature distribution for different radial positions. No insulation. Inductive heating at 190 Watts.

Fig. 4. This is a positive feature of the inductive heating system since it allows reaching greater axial locations of the line without increasing excessively the temperature of the mid section of the line.

The issue just mentioned, related to the uncertainty on the volume in which the power is distributed, is of fundamental importance to the numerical calculations, since the power per unit volume, q''', is a necessary input information. Since no information related to the spatial distribution of the induced power was available in the experiments, no numerical simulations were attempted.

The steady state axial temperature distribution for different radial positions is shown in Fig. 8, for the inductive heating system. The power level delivered is 190 W. The radial temperature uniformity is evident from the data. The temperature at the paraffin/line wall interface is slightly higher than the center line temperature, reaching no more than 33 ^{0}C at x/R = 0.

5.3. Numerical predictions long subsea flexible lines

The reasonable agreement obtained between the experimental and numerical results for the laboratory resistive heating configurations encouraged the utilization of the numerical solutions for predicting the thermal behavior of longer lines plugged with paraffin, as encountered in field applications. In this case, the longer heating sections diminishes the effects of the unknown axial distribution of the inductive power along the steel layer, turning a numerical solution meaningful. The configuration simulated is a section of an infinite line with a 10-meter long plug of solid paraffin. Only the blocked region is simulated. The characteristics of the line are the same as the sample line tested in the laboratory experiments. Following the indication of the laboratory results, the line is isolated along its whole blocked length with a 50-mm thick rubber insulation (k = 0.1 W/m ^{o}C). Heating is provided by a 5-m long induction coil located at the center of the blocked region, which was modeled as a power per unit volume distributed in the carbon steel layer. The external heat transfer coefficient was estimated to be of the order of 300 W/m^2 ^{o}C. The external water temperature was maintained at 5 ^{o}C. The power level used in the calculations was varied until the hottest point in the internal and external polymeric layers reached the maximum allowable value of 90^{o}C. The power level obtained with this procedure was 225 W.

The steady state axial temperature distributions for the center line (r/R =0) and the external polymeric layer (r/R = 1.1) obtained with the calculations are presented in Fig. 9, for half of the line axial length. The temperatures for these two radial positions, and for all other radial positions in between, cannot be distinguished within the accuracy of the plot. The results show that, as in the laboratory tests, only the portion of the line underneath the heating induction coil is heated significantly. Out of this region, despite the use of a complete insulation cover, there is a sharp drop in temperature that would not allow the softening of the solid wax.

Additional simulations of a long line were performed. This time, the whole length of the line was covered with the heating coil. A power of 300 W was applied. This value was the power necessary to heat the wax in the interior of the line to a temperature close to its melting point. The results obtained have shown an axially uniform temperature profile at 60 ^{o}C, for the entire length of the line, and for all layers of the line. These simulations are encouraging results that indicate that, from a thermal point of view, the inductive heating technique is viable. The issue of the technological viability of delivering the power level required to provide the desired temperature levels remains to be studied, and it is beyond the scope of the pres ent work.

6. Concluding remarks

The experiments and numerical calculations reported in the present paper were aimed at studying the thermal viability of using electromagnetic induction to heat subsea flexible lines as a means of removing solid wax plugs that block the lines.

The results obtained indicate that the steel layers that compose the commercial flexible lines can be heated by induction and transfer the heat to the solid wax plug in the interior of the line. A cylindrical heating coil positioned around a sample of a flexible line immersed in cold water was used in the experiments. The heating was shown to be concentrated in a region just under the heating coil, for the case where no thermal insulation was used outside the line.

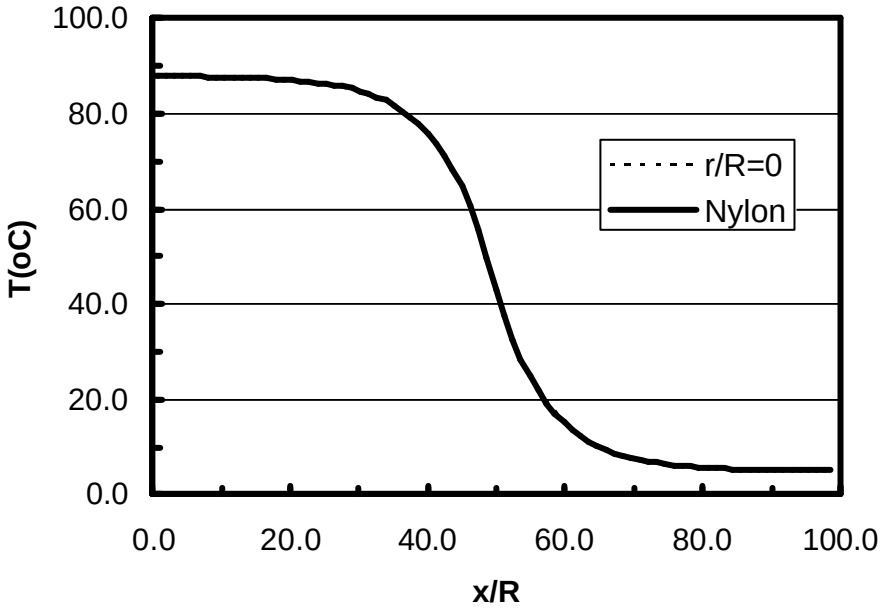

Figure 9– Numerically determined, steady state axial temperature distribution for insulated line. Inductive heating up to x/R = 50.

For the isolated line, the axial temperature distribution was found to be more uniform, allowing the heating of somewhat longer lengths of the line.

Two-dimensional, transient heat conduction solutions were obtained, and shown to agree reasonably well with data from experiments specially designed to validate the numerical calculations. In these experiments, controlled resistive heating was employed to heat the line and the solid paraffin in its interior. It is believed that a better knowledge of the thermophysical properties of the several materials involved in the conduction problem is necessary to improve the level of agreement between experiments and computation.

The numerical solutions were employed to estimate the temperature levels in the layers that compose the flexible line, since no thermocouples were installed in the line wall. These results aided in the choice of the power levels used in the experiments, by indicating the positions where the maximum allowable temperatures in the polymeric layers of the flexible line wall were reached. These temperatures are limiting values that guarantee the integrity of the polymeric materials of the line.

Numerical solutions were also obtained for longer plugged regions of the lines, typically encountered in field applications (around 10-m long). The results indicate that the desired temperature levels to be attained in the paraffin plug in order to allow its removal are only obtained by heating the total length of the blocked region. The power levels necessary to heat these long portions of blocked lines were considered feasible for deep water applications.

As a last comment, it should be mentioned that the cylindrical heating coil was employed in the laboratory experiments to study the concept of inductive heating a commercial flexible line. This geometry, however, is not suited for field applications since it becomes impossible to fit a cylindrical coil around a long line laying at sea bed. Other geometries for the heating are presently being tested.

7. Acknowledgments

The authors gratefully acknowledge the support awarded to this research by the Petrobras R&D Center, in particular to engineers Carlos Dittz and Cássio Kuchpil. Additional support awarded by CTPETRO, the Petroleum Research Fund from the Brazilian Government and ANP, the National Petroleum Agency is acknowledged. Appreciation is extended to Prof. A.C. Bruno from the Physics Department of PUC-RIO for the helpful comments regarding electromagnetic induction. The help from Prof. A.O. Nieckele from the Mechanical Engineering Department of PUC-RIO with the numerical simulations is greatly appreciated. The first two authors acknowledge the scholarships awarded by CNPq, the Brazilian Research Council, and FAPERJ, the Research Foundation of Rio de Janeiro.

8.References

ASHRAE Handbook of Fundamentals, 1981, American Society of Heating, Refrigerating and Air-Conditioning Engineers, Inc., Atlanta.

Dittz, C.H.S., 2001, "Electromagnetic Induction in Flexible Lines Used for Petroleum Transport", Master Dissertation, Physics Department, PUC-RIO, in Portuguese.

Incropera, F.P. and DeWitt, D.P., 1990, Introduction to Heat Transfer, Second Edition, John Wiley and Sons.

Khalil, C.N., Neumann, C.A., Linard C.A. and Santos, I.G., 1994, "Thermochemical Process to Remove Paraffin Deposits in Subsea Production Lines", Proceedings of the Offshore Technology Conference, Houston, pp. 573-579.

Kuchpli, C., 2001, personal communication.

Machado, A.L.C., 1999, "Study of the Influence of Ethylene-Vinyl Acetate (EVA) Copolymers on the Petroleum Flow Properties and Paraffin Deposition Inhibition, Ph.D. thesis, Federal University of Rio de Janeiro – UFRJ, Rio de Janeiro, Brazil (in portuguese).

Patankar, S.V., 1980, Numerical Heat Transfer and Fluid Flow, Hemisphere, New York.

Zinn, S., Semiatin, S.L., 1988, "Elements of Induction Heating Design, Control and Applications, ASM International.